Acta Futura 4 (2011) 81-97
DOI: 10.2420/AF04.2011.81

Acta Futura

Micro-to-Macro: Astrodynamics at Extremes of Length-scale

Colin R. McInnes*, Matteo Ceriotti, Camilla Colombo, Joan-Pau Sanchez
Russell Bewick, Jeannette Heiligers and Charlotte Lücking

Advanced Space Concepts Laboratory, University of Strathclyde, Glasgow G1 1XJ, United Kingdom

Abstract. This paper investigates astrodynamics at extremes of length-scale, ranging from swarms of future 'smart dust' devices to the capture and utilisation of small near Earth asteroids. At the smallest length-scales, families of orbits are found which balance the energy gain from solar radiation pressure with energy dissipation due to air drag. This results in long orbit lifetimes for high area-to-mass ratio 'smart dust' devices. High area-to-mass hybrid spacecraft, using both solar sail and electric propulsion, are then considered to enable 'pole-sitter' orbits providing a polar-stationary vantage point for Earth observation. These spacecraft are also considered to enable displaced geostationary orbits. Finally, the potential material resource available from captured near Earth asteroids is considered which can underpin future large-scale space engineering ventures. The use of such material for geo-engineering is investigated using a cloud of unprocessed dust in the vicinity of the Earth-Sun L_1 point to fractionally reduce solar insolation.

1 Introduction

The growing utilisation of space as a platform for science, telecommunications, Earth observation and navigation is a direct result of the application of the tools of classical orbital dynamics. Many decades of applied research have translated key ideas from dynamical astronomy to spacecraft astrodynamics to generate families of orbits which now deliver essential scientific and commercial products such as high bandwidth data-links, high resolution multi-spectral imagery and precise global positioning. While such exciting space applications have transformed a range of both commercial and public services, the continued exploitation of space will require new innovations both in spacecraft technologies and in fundamental astrodynamics.

This paper provides an overview of an on-going programme of work which aims to deliver radically new approaches to astrodynamics at extremes of length-scale to underpin new space-derived products and services for space science, telecommunications and Earth observation. These include vast swarms of interacting MEMS-scale 'smart dust' devices for new science applications [9, 23], displaced polar and geostationary orbits for Earth observation and communications [6, 15] and new concepts for the capture and exploitation of small near Earth asteroids [33, 3], as illustrated schematically in Fig. 1.

Traditionally, astrodynamics has centred on the classical gravitational two-body problem, with additional forces treated as small perturbations. This approach allows the conic section solutions to the unperturbed gravitational two-body problem to form the basis of an understanding of the weakly perturbed problem (for example [18, 31]).

*E-mail address: colin.mcinnes@strath.ac.uk

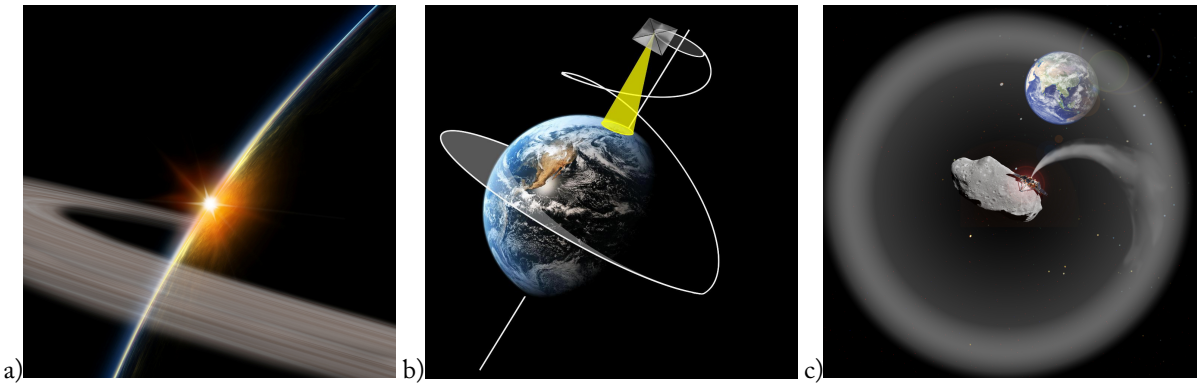

Figure 1. *Micro-to-macro: future space systems at extremes of length-scale (a) MICRO: swarms of 'smart dust' sensor nodes (b) MESO: pole-sitter orbits for gossamer spacecraft (c) MACRO: geo-engineering with captured near Earth asteroid material.*

Such an approach has provided the mathematical tools to enable, for example, orbit control of geostationary telecommunication satellites, the definition of mapping orbits for Earth observation satellites and coverage patterns for satellite navigation constellations.

More recently, the use of modern dynamical systems theory has led to exciting new developments in the gravitational three-body problem (for example [19, 13]). Work has explored the use of new families of trajectories connecting periodic orbits about the collinear libration points as the basis for highly efficient orbit transfer in the Earth-Moon and Earth-Sun systems. These more recent developments are a strong indication that there is much work still to be done in modern astrodynamics, and that many new families of useful orbits await discovery.

Future space systems will require a new approach to orbital dynamics from micro- to macroscopic length-scales L. This new understanding will be required to underpin the exploitation of future space systems from swarms of interacting MEMS-scale 'smart dust' devices ($L \sim 10^{-3}$ m) to extremely large gossamer spacecraft ($L \sim 10^{3}$ m). At these extremes of spacecraft length-scale, perturbations such as atmospheric drag, solar radiation pressure and electrodynamic forces can be of the same order of magnitude as the central two-body or three-body gravitational forces. The strongly perturbed nature of the dynamics of such spacecraft gives rise to rich new families of orbits which can be exploited to deliver new space products and services.

Gossamer spacecraft are characterised by a large deployable surface area, but a relatively modest mass, yielding extremely low areal densities. These spacecraft are strongly perturbed by atmospheric drag and solar radiation pressure, and in the case of solar sails, utilise solar radiation pressure directly for propulsion. Similarly, micro-spacecraft are rapidly shrinking in mass and volume, driven by advances in integrated microelectronics. Since spacecraft mass scales as L^3, while surface area scales as L^2, effective areal density scales as L^{-1} with diminishing spacecraft size. This again leads to strong atmospheric drag and solar radiation pressure perturbations and the possibility of electrodynamic effects due to natural or artificial surface charging. Therefore both classes of spacecraft, while at opposing ends of the length-scale spectrum, will require the integrated development of new methods in astrodynamics to explore such strongly perturbed orbits. At even larger length-scales, new insights into the three-body problem can enable the capture of small near Earth asteroids by greatly leveraging the effect of intervention by impulse or continuous thrust. The ability to efficiently capture such material could have a long-term impact on the feasibility and cost of future space systems at the largest length-scales such as space solar power and space-based geo-engineering.

Key questions to be addressed in each of the following three sections include:

- MICRO: How does the orbital dynamics of micro-spacecraft scale with rapidly diminishing spacecraft size and how can the orbits of swarms of such devices be controlled?
- MESO: Can different natural perturbations and low thrust propulsion technologies be combined to

 DOI: 10.2420/AF04.2011.81

enable new families of exploitable orbits for large gossamer spacecraft?

- MACRO: Can new insights from orbital dynamics bring forward the development of visionary, large-scale space engineering ventures by efficiently capturing near Earth asteroid resources?

2 MICRO: Astrodynamics for *smart dust* swarms

2.1 Long-lived orbits for smart dust devices

Recent innovations in spacecraft design have exploited advances in miniaturisation to fabricate small satellites with dimensions of a single micro-chip. Low-cost manufacturing of vast numbers of micro-spacecraft can lead to their use in swarm applications, and their small dimensions facilitate access-to-space through deployment in orbit as piggy-back on a conventional spacecraft. The deployment of vast numbers of *'SpaceChips'* will enable future missions, such as global sensor networks for Earth observation and communication, distributed space missions for multi-point, real-time sensing for space science, interplanetary exploration in support of traditional spacecraft, deployment in the vicinity of a spacecraft for environmental and damage detection, or possibly future space-based geo-engineering applications. Even if limited, micro-spacecraft are also capable of long-term orbit control through the exploitation of perturbations such as Lorentz force, solar radiation pressure or atmospheric drag and vicinity control by means of spacecraft-to-spacecraft interaction through the Coulomb force.

Moreover, the exploitation of orbital dynamics at extremely small length-scales can enable novel families of exploitable non-Keplerian orbits. Due to the extremely high area-to-mass ratio (A/m) of future SpaceChips, or smaller *'smart dust'* devices, with respect to conventional spacecraft, perturbations such as solar radiation pressure (SRP) and aerodynamic drag, which goes as A/m, become dominant with respect to the Earth's gravity. The study of the long-term effect on the satellite's orbit caused by those perturbations generates equilibrium orbits where the total variation of semi-major axis and eccentricity due to SPR and drag is zero, and the effect of SRP is exploited to obtain Sun-synchronous precession of the apse-line passively, without the use of active control. In those regions of the orbital element phase space where solar radiation pressure and atmospheric drag both have a non-negligible effect on the spacecraft orbit, complete equilibrium is not possible. However, the long-term orbit evolution still presents some intriguing behaviour; if the initial conditions are in a certain region around the equilibrium solution set, the long-term evolution is characterised by librational motion, progressively decaying due to the non-conservative effect of atmospheric drag [11, 10] (see Fig. 2). It is possible to define different arcs of the orbit evolution where the trajectory is dominated either by drag or by solar radiation pressure.

The natural effects of solar radiation pressure and atmospheric drag perturbations can be exploited to design swarm missions, for example, for the mapping and study of the upper regions of the Earth's atmosphere [9]. A swarm of SpaceChips is deployed on the ecliptic plane from a single spacecraft, as distributed nodes of a network to obtain a spatial and temporal map of the ionosphere and exosphere. By selecting the release conditions in terms of angular displacement ϕ between the orbit pericentre and the direction of the Sun-Earth line, the effect of SRP is exploited to scatter the devices into a set of different orbits which cover an extended, but bounded, region of the atmosphere, collecting distributed measurements.

Figure 2 shows the long-term evolution of the SpaceChip swarm after release from a conventional spacecraft. For the first part of the orbit evolution for $\phi < \pi$ the secular rate of change of the eccentricity is negative; as a consequence the orbit perigee rises reaching its maximum at $\phi = \pi$. Afterwards, when $\phi > \pi$, the secular variation of eccentricity is negative, hence the perigee height decreases.

Importantly, the short lifetime of high area-to-mass spacecraft can be greatly extended (and indeed selected) through the interaction of energy gain from asymmetric solar radiation pressure and energy dissipation due to drag (see blue line in Fig. 6). Due to the large area-to-mass ratio of these devices orbit lifetime due to air drag alone is extremely short (see green lines in Fig. 2 and Fig. 6). In addition, the effect of atmospheric drag can be exploited to obtain a fast decay of the swarm of devices in the terminal phase of the mission, ensuring their end-of-life disposal and avoiding the creation of long-lived space debris from the swarm.

More intriguing new behaviours are found when planet's oblateness is considered in the governing equations and the motion is not bounded to the ecliptic plane.

DOI: 10.2420/AF04.2011.81

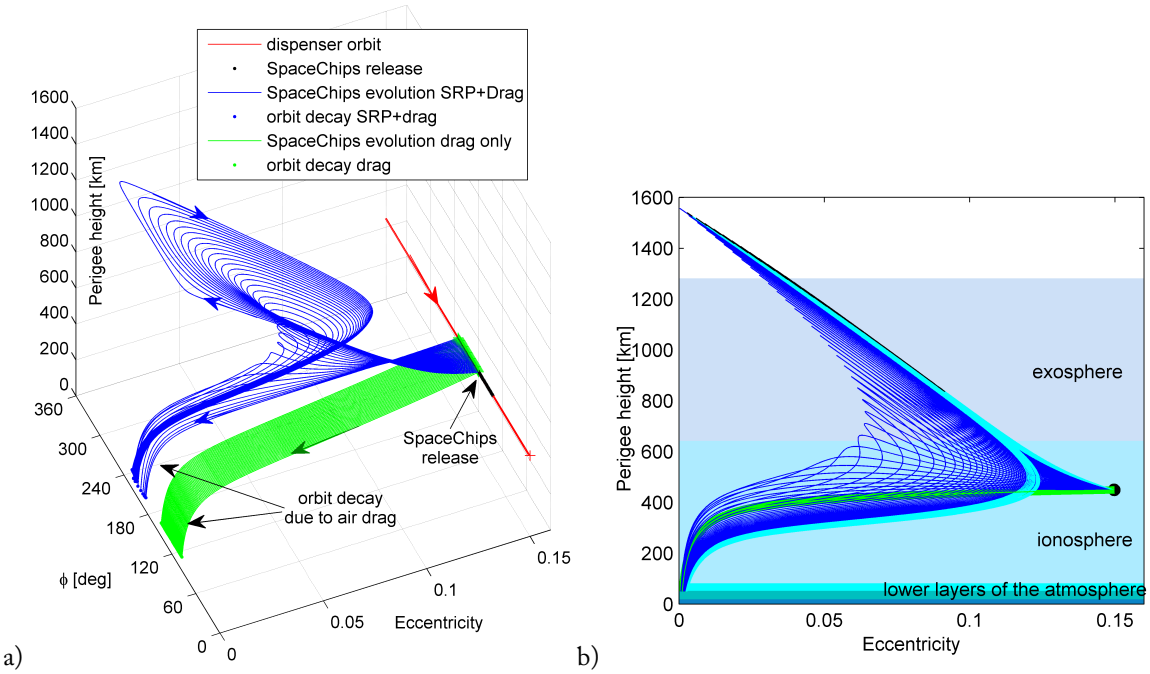

Figure 2. *SpaceChip swarm mission. As a conventional dispenser spacecraft moves on its orbit (red), it releases a number of SpaceChips, whose long-term evolution under the effect of SRP and drag is represented by the blue line. The long-term evolution under drag only is represented with the green line. (a) Orbit evolution in the phase space. (b) Atmosphere coverage in the eccentricity-perigee height plane. The exploitation of SRP allows coverage of a more extended region of the atmosphere from the device release (black point) until the final decay (when the perigee height decreases below 50 km).*

2.2 Electrochromic orbit control of high area-to-mass ratio spacecraft

Possible mission concepts for swarms of 'smart dust' devices can be extended by including active orbit control over the long-term evolution of the swarm. An electrochromic coating of the SpaceChip device can be employed to alter the reflectivity coefficient of the spacecraft. This control method is intended primarily for micro-scale satellites-on-a-chip that do not possess the physical size for conventional orbit control actuators such as thrusters and have a naturally high area-to-mass-ratio. However, larger satellites could also exploit these findings by employing a large lightweight inflatable balloon with an electrochromic coating. Electrochromic materials are already widely used in terrestrial applications such as intelligent sunshades, tinting windows and flexible thin film displays and have been used in space applications, albeit not for orbit control. The recently launched IKAROS solar sailing demonstrator uses electrochromic surfaces on the sail to adjust its attitude and electrochromic radiators have been developed for thermal control. Electrochromic materials (EM) change their optical properties when a voltage is applied, thus modulating the fraction of light which is transmitted, absorbed and reflected, therefore effectively changing the reflectivity coefficient c_R of the spacecraft between two set values ($c_{R\,min} = 1$ and $c_{R\,max} = 2$). The acceleration any object receives from the solar radiation pressure is given by:

$$a_{SRP} = c_R \frac{p_{SR}}{c} \frac{A_\odot}{m} \tag{1}$$

where c_R is the coefficient of reflectivity, p_{SR} the solar flux, c the speed of light, $A_\odot$ the effective surface area receiving solar radiation and m is the mass of the object. It can be seen that the value of a_{SRP} in Eq. (1) depends on the area-to-mass ratio of the object. Conventional spacecraft experience SRP only as a perturbing force whereas the effect on micro-scale satellites becomes dominant. Because of the discrete nature of the reflectivity change, the orbit control has the characteris-

 DOI: 10.2420/AF04.2011.81

tics of a on-off controller with the lower reflectivity state ($c_{R\,min}$) of the EM thin-film defined as the off-state and the higher reflectivity state ($c_{R\,max}$) as the on-state. It is assumed that during each orbit the reflectivity can be switched twice. The true anomalies at which these changes take place are used as control parameters.
Through this control method the effect of SRP can be modulated to stabilise the spacecraft in certain sun-synchronous, elliptical orbits and orbital manoeuvres can be performed [23]. For stabilisation, an artificial potential field controller has been implemented using a quadratic potential in the orbital element phase space around the desired stabilisation point. A region in the eccentricity-ϕ-phase-plane has been identified where spacecraft could be stabilised indefinitely. For orbital manoeuvres, instead, the electrochromic control method is used to balance the effect of eclipses to keep a constant semi-major axis. There are two possible solutions achieving this, by maintaining the reflectivity mainly low or mainly high along each single orbit revolution. This choice will determine the set of flow lines the spacecraft will follow in the phase space. Each member of the swarm can be thus navigated, depending on its current position in the phase space with respect to the targeted final position.
The results of a case study are shown in Fig. 3; eight SpaceChips starting from different initial orbits are collected into the same final orbit within one year using electrochromic orbit control. On the left the initial and final orbits are displayed. The right figure shows the evolution of the eccentricity, ϕ, over time, while the semi-major axis remains constant, and the centre figure shows the evolution of the orbits in the phase plane. The spacecraft start on the orbits marked by the coloured circles and then progress following the flow lines towards the goal orbit marked with a black circle. The dashed flow lines correspond to the higher reflectivity control option, the dotted lines to the lower reflectivity control option.

2.3 Extension of the mission design through active control of the swarm

The mission concepts presented in Section 2.1 can be extended by including active orbit control over the long-term evolution of the SpaceChip swarm [8]. The control relies on a basic bang-bang control algorithm based on a simplified version of the electrochromic orbit control introduced in Section 2.2. The spacecrafts follow the natural flow lines in the orbital element phase space for the major part of their evolution accepting a change in semi-major axis due to eclipses. The change of reflectivity coefficient takes place every time the angle between the orbit pericentre and the direction of the Sun-Earth line ϕ goes through π (see Fig. 4)

$$c_R = \begin{cases} c_{R\,max}, & \text{if } \phi < \pi \text{ and } t \leqslant T_{mission\,max} \\ c_{R\,min}, & \text{if } \phi \geqslant \pi \text{ and } t \leqslant T_{mission\,max} \\ c_{R\,max}, & \text{if } t > T_{mission\,max} \end{cases} \quad (2)$$

In this way the long-term control of the orbit can be achieved and a swarm of SpaceChips moving along different librational loops can be stabilised in the phase space at $\phi = \pi$, with an eccentricity within a certain range. Once the stabilisation region is reached, the spacecraft will change its reflectivity value, once per orbit, thus keeping its orbital elements fixed in a position of the phase space which, otherwise, will not be in equilibrium. To avoid the debris hazard of the swarm existing for an indefinite time, the duration of the mission is limited to a maximum value $T_{mission\,max}$, after which the control algorithm is turned off and the swarm naturally evolves towards a fast decay, due to the effect of atmospheric drag.
Figure 5 shows the evolution of the perigee heights with time. The passive exploitation of SRP (blue lines) allows an increase of the perigee height and an extension of the lifetime with respect to the drag-only scenario (green lines). The control strategy (red lines) for the reflectivity coefficient allows stabilising the members of the swarm at a constant perigee for a long duration. Importantly, the effect of SRP causes a significant increase in the orbit lifetime with respect to the drag-only case, as shown in Fig. 6, as a function of the angular displacement at release. The green line represents the orbit lifetime of the swarm in the case SRP is not considered, and the blue line corresponds to the passive evolution under drag and SRP with a constant value or reflectivity $c_R = c_{R\,max}$. If the control strategy in Eq. 2 is implemented, the swarm lifetime is shown with the red line.

3 MESO: Astrodynamics for gossamer spacecraft

The orbital dynamics of a large, high-area-to-mass ratio spacecraft is greatly influenced by natural perturbations, generating new kinds of exploitable orbits. For example, non-Keplerian orbits (NKO) are those in which a small, but continuous acceleration is used to generate

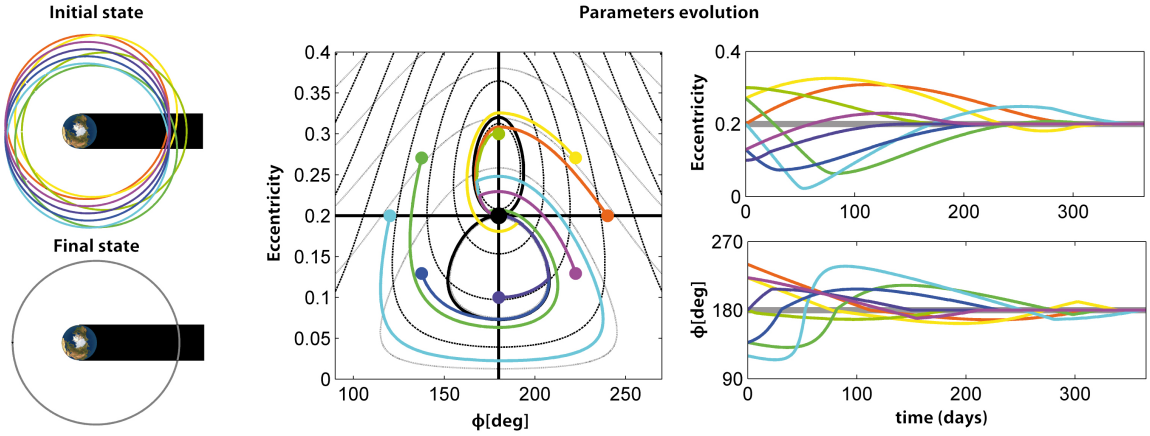

FIGURE 3. *Results of a case study simulation for the electrochromic orbit control. Initial and final orbital state of eight spacecraft and evolution of their orbital parameters in the e-ϕ-phase space and over the time of the simulation (1 year).*

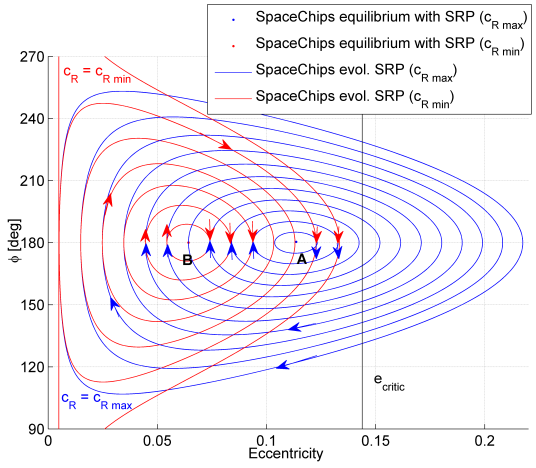

FIGURE 4. *Schematic of the control algorithm based on the reflectivity coefficient change.*

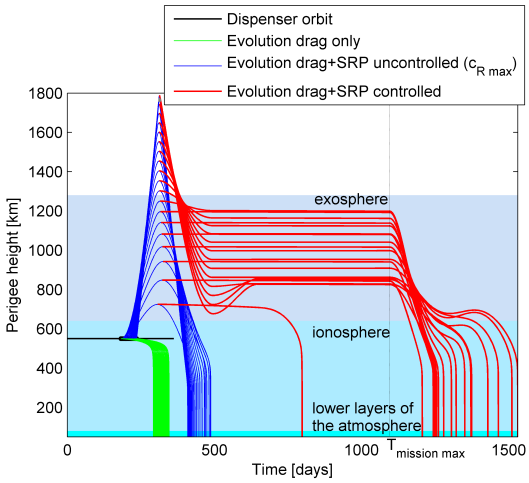

FIGURE 5. *Evolution of the swarm under the effect of drag-only (green lines), drag and SRP uncontrolled (blue lines), drag and SRP controlled (red lines).*

periodic orbits that do not follow the natural dynamics of the system [26]. Both solar sailing [2] and solar electric propulsion (SEP) [25] have been proposed as technologies to enable these kind of missions. However, we propose to hybridise the two technologies on a gossamer spacecraft [21], and investigate the advantages.

In the hybrid spacecraft, the sail is fixed on the spacecraft bus and its thrust is controlled by changing the sail attitude. Solar arrays or thin film solar cells (TFSC) partially covering the sail surface are used to power the SEP thruster. This is assumed to be mounted on a gimbal, such that the direction of its thrust can be controlled.

At the cost of increased spacecraft complexity, the two separate propulsion systems complement each other, cancelling their reciprocal disadvantages and limitations. In principle, a steerable SEP thruster can provide the missing acceleration component (towards the Sun) that the sail cannot generate. Similarly, the hybrid spacecraft can be seen as an SEP spacecraft, in which an auxiliary solar sail provides part of the acceleration, en-

 DOI: 10.2420/AF04.2011.81

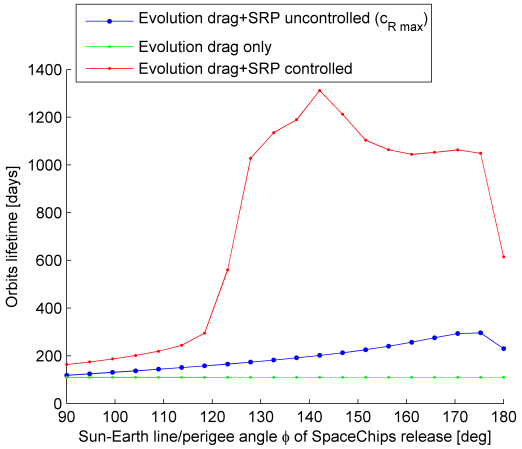

Figure 6. *Orbit lifetime as function of the angular position of SpaceChips release.*

abling saving of propellant and a lower demand on the electric thruster, possibly with some intervals in which it could be turned off. In this sense, the hybrid spacecraft can be seen as a way to gradually introduce solar sails for space applications [29], and hence to reduce the advancement degree of difficulty (AD2) [24] in the technology readiness level scale.

To maximise the performance of the hybrid spacecraft, the objective is to minimise the SEP propellant consumption. When the position, velocity and mass of the spacecraft are known at a particular instant of time, the acceleration due to gravitational forces (that need to be counterbalanced by the hybrid propulsion) can be computed, and thus the problem is to find the optimal solar sail cone and clock angles α, δ such that the SEP acceleration a_T is minimised [5]:

$$(\alpha^*, \delta^*) = \arg\min\left(a_T\left(\alpha, \delta\right)\right) \tag{3}$$

By exploiting this method, this section investigates the application and advantages of hybrid propulsion for two types of NKO: optimal Earth pole-sitter orbits and displaced geostationary orbits.

3.1 Optimal Earth pole-sitter orbits

A pole-sitter is a spacecraft that is constantly above one of the Earth's poles, i.e. lying on the Earth's polar axis [12]. This type of mission could provide a continuous, hemispherical, real-time view of the poles, and will enable a wide range of new applications in climate science and telecommunications [20].

We consider the Sun-Earth circular restricted three-body problem (CR3BP). Since the polar axis of the Earth is almost fixed while the Earth rotates around the Sun, in the synodic reference frame, it appears to span a full conical surface of half angle 23.5 deg every year. The spacecraft has to follow the same motion during its mission, and this can therefore be translated into constraints on the position as a function of time (see Fig. 7).

We seek optimal periodic pole-sitter orbits that exploit the solar sail to minimise the SEP propellant consumption over a fixed period (one year), while maintaining the pole-sitter condition at each instant during the mission. Optimal orbits are defined in terms of evolution of the states (position, velocity, mass), and controls (sail cone and clock angles, SEP thrust direction and magnitude) over one year. The optimal orbit design is performed in two steps. In the first step, after assigning a trajectory that satisfies the pole-sitter constraints, a locally-optimal control history is found, through a semi-analytical procedure, solving the problem in Eq. 3. This solution is then used for initialising the second step, which optimises the first guess through a pseudospectral transcription of the optimal control problem. Details of the design and optimisation process are covered in [5].

The analysis is done for both the pure SEP spacecraft, and the hybrid spacecraft in a range of system lightness numbers β_0, which is proportional to the area-to-mass ratio of the hybrid sailcraft, and hence a measure of the sail size for a given initial mass.

First, it is found that a consistent gain in propellant mass fraction is obtained by adding a small sail to a pure SEP spacecraft. As the lightness number increases towards very high values, the gain in propellant mass for a given increase of β_0 becomes less. However, this fact justifies the investigation of the hybrid spacecraft, seen as a pure SEP system with a small-lightness-number auxiliary sail.

If the distance of the spacecraft from the Earth is kept constant (an example of such an orbit is in Fig. 8), it is found that an optimal distance exists at which the propellant consumption is minimised. This distance is approximately 0.018 AU (or about 2.7 millions of km), depending on the lightness number, and is of the same order as that of the Lagrangian point L_1 of the Earth-Sun system (1.5 million km from the Earth).

Note that the distance from the Earth can be varied: this degree of freedom can be used to find novel families of optimal orbits, leading to additional propellant mass saving. Different optimal orbits are found depending on

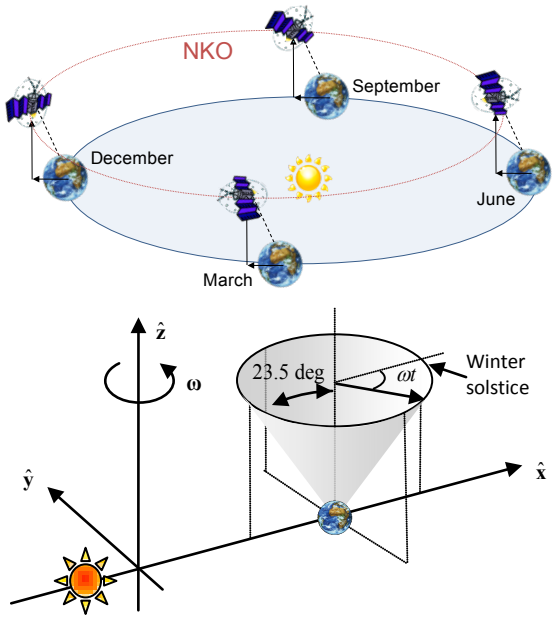

Figure 7. *Apparent precession of the Earth's polar axis due to rotation of reference frame. (a) Inertial frame. (b) Synodic frame.*

the value of β_0. Optimal orbits get closer to the Earth in winter and farther in summer, as the lightness number of the solar sail increases. The distance can even double from winter (2 million km) to summer (4 million km) for a hybrid spacecraft with a lightness number of 0.1 (Fig. 9).

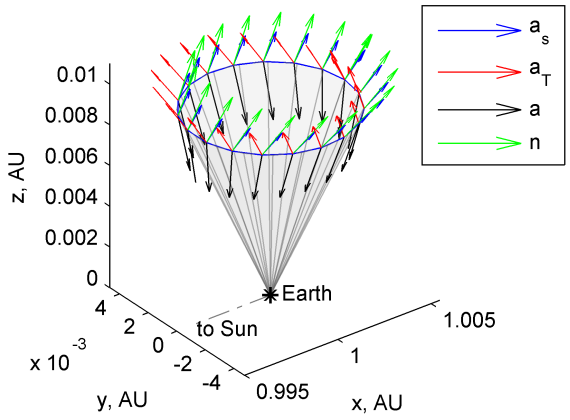

Figure 8. *Sail acceleration (α_s), SEP acceleration (α_T), total gravitational acceleration (α) and sail normal (n) on a constant-distance orbit at 0.01 AU.*

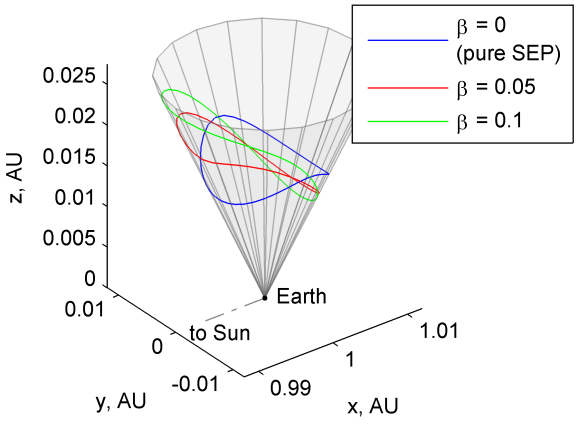

Figure 9. *Minimum propellant mass hybrid pole-sitter orbits, for three different values of β_0*

DOI: 10.2420/AF04.2011.81

By comparing optimal solutions for pure SEP and hybrid spacecraft, it is found that the latter requires a lower propellant mass fraction. A substantial saving in propellant is obtained by adding a relatively small sail: considering an initial mass of 1000 kg, an SEP specific impulse of 3200 s and an optical sail model, for a 1-year orbit, the propellant mass decreases from 158 kg (for the pure SEP) to 97 kg ($\beta_0 = 0.05$).

However, the hybrid spacecraft is a more complex system, mainly due to the presence of the solar sail and the need for a gimballed thruster. Therefore, a preliminary systems design is performed, to assess the conditions at which the hybrid spacecraft is advantageous over the conventional SEP one, in terms of a lower initial mass for carrying the same payload mass.

It is found that, with near- to mid-term sail technology (sail loading of 7.5 g/m^2), the hybrid spacecraft has a lower initial mass than the SEP case if the mission duration is 7 years or more, with greater benefit for longer missions. Assuming far-term sail technology (5 g/m^2), then the hybrid spacecraft outperforms the pure SEP case even for short missions [7]. The comparison is performed varying the distance from the Earth optimally for each type of spacecraft.

Due to the instability of pole-sitter orbits, a feedback control is necessary to keep the spacecraft on track, counterbalancing errors and small perturbations that are not considered in the dynamics for the reference solution, as well as errors in the spacecraft model (e.g. unpredictable degradation of the sail). It was shown [6] that it is possible to keep the spacecraft on-track, and counterbalance injections errors, only by using the SEP thruster, while maintaining the sail at nominal attitude. Furthermore, it was shown that a relatively small variation of the reference thrust vector is sufficient to respond to large injection errors (order of 100,000 km), and to recover from relatively long SEP failures (up to 35 days).

3.2 Displaced geostationary orbits

With a period equal to the Earth's rotational period, spacecraft in geostationary orbit (GEO) are stationary with respect to their ground station, allowing for a continuous downlink to Earth. Vital telecommunication and Earth observation satellites are currently exploiting this unique property of the geostationary orbit. However, due to limits imposed by east-west spacing requirements, the GEO is starting to get congested at certain key longitude slots [17]. Therefore, in order to increase its capacity, we propose the use of displaced NKOs.

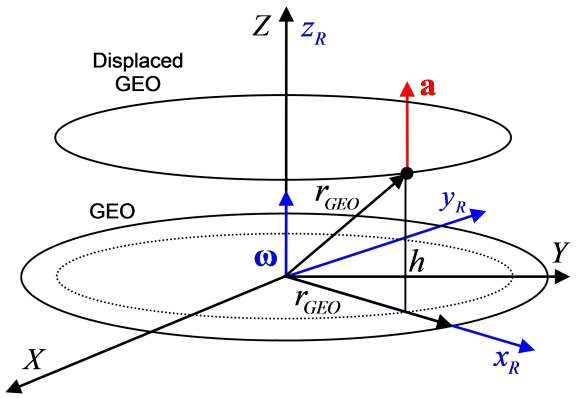

Figure 10. *Definition of displaced geostationary orbit (GEO)*

By applying a continuous acceleration to counterbalance the gravitational acceleration, the geostationary orbit can be levitated above or below the equatorial plane, thereby creating new geostationary slots. Pure solar sailing has already been considered to maintain such displaced geostationary orbits, but a residual force in the equatorial plane causes the spacecraft to move with respect to its ground station. Furthermore, only small displacements, still inside the geostationary station keep box, appeared to be feasible, causing collision risk to spacecraft in the geostationary orbit [2]. To overcome these problems, we propose to maintain the displaced GEO using hybrid propulsion.

We can find displaced geostationary orbits, or displaced NKOs in general, by seeking equilibrium solutions to the two- or three-body problem in a rotating frame of reference. A transformation to an inertial frame will subsequently show that the spacecraft executes a circular orbit displaced away from the centre of the central body [26].

The situation as it occurs in the displaced geostationary orbit is depicted in Figure 10: the geostationary orbit is levitated over a distance h while keeping both the orbital radius and the orbital angular velocity equal to the orbital radius and orbital angular velocity in the geostationary orbit, r_{GEO} and ω respectively. This case corresponds to a so-called 'Type I' NKO for which the required thrust induced acceleration is at its minimum [27]. The direction of the required acceleration is pure out-of-plane and, for the displaced GEO, the magnitude is solely a function of the displacement distance h.

With the required acceleration known, the minimisation problem in Eq. 3 can be solved for a particular value

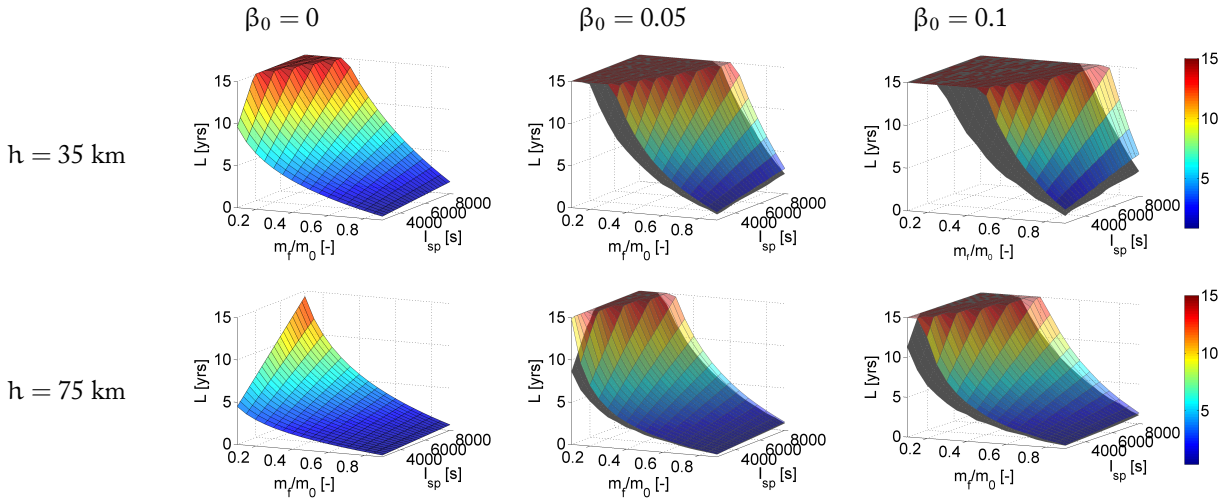

Figure 11. *Mission lifetime* L *as a function of the specific impulse* I_{sp} *and the mass fraction* m_f/m_0*, for different values of the system lightness number* β_0 *and the displacement distance* h*. The coloured surfaces include a seasonal transfer between a geostationary orbit displaced above and below the equatorial plane. The grey surfaces exclude this transfer.*

for h. Analytical formulae for the optimal steering law are found by setting the partial derivative of the SEP acceleration with respect to the sail pitch and yaw angles equal to zero and requiring that the second derivative is positive. As mentioned, Eq. 3 can be solved at a particular instant in time, i.e. for a given value for the mass and given time during the year. The latter is related to the change in the direction of the Sun-sail line due to the tilt of the Earth's rotational axis with respect to the ecliptic plane. By using a discretisation of the orbit into equally distributed nodes, the analysis described can be extended to find the variation of the SEP and solar sail controls and accelerations, SEP thrust magnitude and spacecraft mass as a function of time over multiple orbital periods [15].

Performing this analysis provides the results as shown in Figure 11, where the performance of the hybrid spacecraft is expressed through the mission lifetime, L. This lifetime is dependent on the amount of propellant onboard the spacecraft, which is represented by the spacecraft dry mass fraction, m_f/m_0, with m_0 the initial spacecraft mass and m_f the spacecraft mass after time L. The figure shows that a wide range of SEP specific impulses are considered. Furthermore, considering a standard geostationary station keeping box of 0.05°-0.1°, equalling 36.8 - 73.6 km, two different displacement distances of 35 and 75 km are investigated. Finally, three different values for the system lightness number are adopted, including the case where $\beta_0 = 0$, which represents the use of pure SEP propulsion and is used for comparison.

Figure 11 shows that, for example, for a 35 km displaced orbit, a currently feasible specific impulse of 3200 s and a mass fraction of 0.5, a lifetime of 3.5 years can be achieved for the pure SEP case, which increases to 9.7 and 15 years for hybrid propulsion, depending on the value chosen for β_0. A slight decrease in the performance can be observed for the higher displaced orbit as for similar values for the specific impulse and mass fraction, lifetimes of 2.9 and 4.3 years can be achieved. Note that these results assume an SEP transfer between a geostationary orbit displaced above the equatorial plane and an orbit displaced below the equatorial plane twice a year, in spring and in autumn, to make full use of the annual changing Sun-sail line direction. Solving the accompanying optimal control problem using a direct pseudo-spectral method shows that this transfer requires an almost negligible propellant budget. To show the influence of this transfer on the performance of hybrid propulsion, Figure 11 also includes the results when the hybrid spacecraft is maintained above the equatorial plane throughout the year. Then, a decrease in the lifetime of a few months up to a few years can be observed, but still exceeds the lifetimes of a pure SEP mission.

To investigate whether the mass fractions and specific impulses of Figure 11 allow for a payload to be carried

 DOI: 10.2420/AF04.2011.81

during the lifetimes shown in those figures, a preliminary spacecraft mass budget is considered to express the performance of the hybrid spacecraft in terms of payload mass capacity. For this, a maximum initial mass, such that the thrust magnitude does not exceed 0.2 N during the mission lifetime, is assumed. Further details on the mass breakdown and technological assumptions can be found in [15]. The results are shown in Figure 12. Considering a lifetime of 10-15 years for current geostationary spacecraft, Figure 12 shows that only hybrid propulsion enables such lifetimes while still allowing for useful payload masses of 255 to 489 kg to be carried on board in a 35 km displaced orbit, while reasonable lifetimes with somewhat smaller payloads can be obtained for the larger displacement of 75 km.

4 MACRO: Astrodynamics for visionary concepts

The final research theme aims to perform speculative research from a level-headed perspective in order to map out possible long-term futures for the utilisation of space by exploiting new insights into astrodynamics. Examples of this speculative research are space-based geo-engineering and asteroid capture and exploitation.

The current consensus within the scientific community is that global warming is currently happening due to the large quantities of greenhouse gases such as CO_2 and methane that are emitted into the atmosphere. It is clear from the slow movement of international agreements on emission restrictions that, should emission caps be put in place, they may be too late to prevent the Earth from warming above the $1.5 - 2.5\,^{\circ}C$ that many fear could cause irreversible effects [16]. Hence it is prudent to investigate possible methods to mitigate the effects of global warming by the deliberate manipulation of the Earth's climate. This field is generally referred to as geo-engineering or climate engineering.

Many proposals have been made for possible geo-engineering schemes and have been evaluated in a study by the Royal Society in 2009 [34] based on affordability, timeliness, safety and effectiveness. The report concludes that currently too little is known about the possible consequences of the these methods to recommend a single system, but also that the best method of implementation is likely to be a mixture of different methods. Aspects of this research theme aims to improve the ability of one of these methods, space-based geo-engineering, to mitigate the worst effects of climate change.

a)

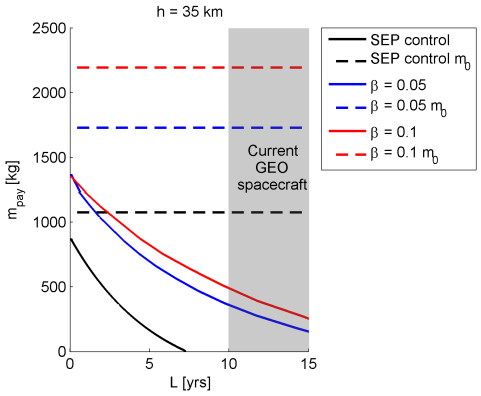

b)

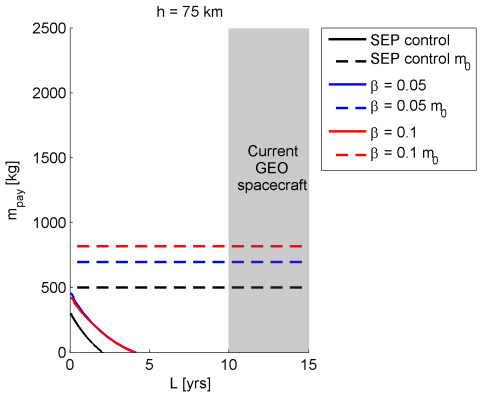

Figure 12. *Payload mass* m_{pay} *as a function of the mission lifetime* L *for different values of the system lightness number* β_0 *and for* I_{sp} *=3200 s. (a) 35 km displacement. (b) 75 km displacement.*

Several scenarios for space based geo-engineering platforms have already been identified [1, 28, 30, 35]. All of these possible solutions require an enormous engineering effort comparable only to the largest engineering ventures on Earth (e.g., Three Gorges dam or Panama Canal), but in a much more hostile environment. However, the level of the engineering undertaking necessary for space geo-engineering, as well as for other future space applications such as space solar power satellites and space tourism, may be relieved to some extent by utilising materials that are already available in space [33].

4.1 Capture of near Earth asteroid material

Small celestial objects, i.e., asteroids and comets, have long been identified as possible reservoirs of materials for utilisation in space. Some examples of this are volatiles for propellant, water for life support, metals for structures, semiconductors for solar cells or simply regolith for radiation shielding [22]. In particular, near Earth asteroids (NEA) have recently risen in prominence because of two important points: they are among the easiest celestial bodies to reach from the Earth and they may represent a long-term threat. A range of methods have also been identified as able to provide a change in the asteroid linear momentum, sufficient to deflect an asteroid on a collision trajectory with the Earth [32]. Using these methods, a resource-rich asteroid could in principle be manoeuvred and captured into a bound Earth orbit through judicious use of orbital dynamics.

The capture and transport of the entire NEA into an Earth orbit, for posterior processing, would require more energy than the transport of processed material directly from the unperturbed asteroid orbit. However, the mining and processing of materials in-situ would entail very complex and long duration missions. Both of these scenarios, in-situ processing and transport or asteroid capture, imply different mission architectures and the optimality of one option with respect to the other may ultimately depend on the technology readiness of the different mission systems, as well as the orbit of each particular asteroid and resource to be exploited. Nevertheless, the required Δv, as a measure of specific energy, is a good figure of merit that provides a qualitative estimate of the required scale of engineering necessary for any of the two options. The question that arises then is how much near-Earth asteroid material is there which could be captured with a modest investment of energy.

This latter question can be answered by comparing the accessible Keplerian orbital regions with a NEA model able to predict the statistical probability of the existence of an asteroid with a given set of orbital elements and diameters (see Fig. 13). The accessible Keplerian region can be delimited by defining a multi-impulsive Keplerian transfer parameterised by the transport cost parameter Δv. The simplest transfer can be modelled by two impulses: first, a change of plane in order to yield a coplanar encounter with Earth, which ensures that if the asteroid is an Earth-crossing object, this would actually cross the Earth's orbital path, and second, a final insertion burn that takes place at the periapsis passage of the Earth encounter. This transfer, as with a Hohmann transfer analysis, provides a good conservative estimate of the exploitable asteroid material. A capture transfer that considers only one single impulse during the periapsis passage of the asteroid can also be modelled. For this second transfer, one needs to compute the subset of asteroids with a given semi-major axis, eccentricity and inclination set $\{a,e,i\}$ that have an orientation such that a serendipitous fly-by with the Earth is possible. Figure 13, for example, shows the accessible volume of the $\{a,e,i\}$ Keplerian subspace considering a one-impulse capture with a Δv threshold at 2.37 km/s, the value required to escape lunar gravity, used to provide a comparison of energy investment [33]. The NEA density distribution is computed by interpolating the theoretical distribution published by Bottke et al. [4] and can also be seen in Fig. 13.

One can then assess the availability of asteroid material on easily accessible orbits by computing the median diameter of the object that can be found within a given Δv limit. Figure 14 shows the median diameter of the first, tenth, hundredth and thousandth largest accessible asteroid in the near Earth space, together with the 90% confidence region for each one of these objects. While the median diameter indicates that there is 50% chance that the i^{th}-largest accessible asteroid could be larger or smaller than the median diameter, the confidence region provides a cumulative 90% chance to find an object size within the shaded area. Finally, the figure also shows the expected median diameter of the accessible objects when the maximum transfer time is set to 40 years. The information in the figure can be read as follows: let us, for example, set the Δv threshold at 100 m/s, the largest accessible object has a 50% probability to be equal to or larger than 24 meters diameter, while we can say with 90% confidence that its size should be between 72 meters and 12 meters. These results are computed assuming a phase free transfer, while if a random, but fixed initial phase is assumed, and 40 years of transfer time are allowed, then the result of the median diameter decreases to 23 meters. The following set of data in the decreasing ordinate axis is the group referring to the 10^{th} largest object found within the region of feasible capture given by a Δv threshold of 100 m/s, whose median diameter is at 8 meters diameter. The 100^{th} largest object is foreseen to have a diameter of 3 meters and 1000^{th} largest of 1 meter.

The results shown in the latter figure highlight the feasibility of future asteroid resource utilisation. One can imagine advantageous scenarios for space utilisation from the results on the expected size of the accessible

 DOI: 10.2420/AF04.2011.81

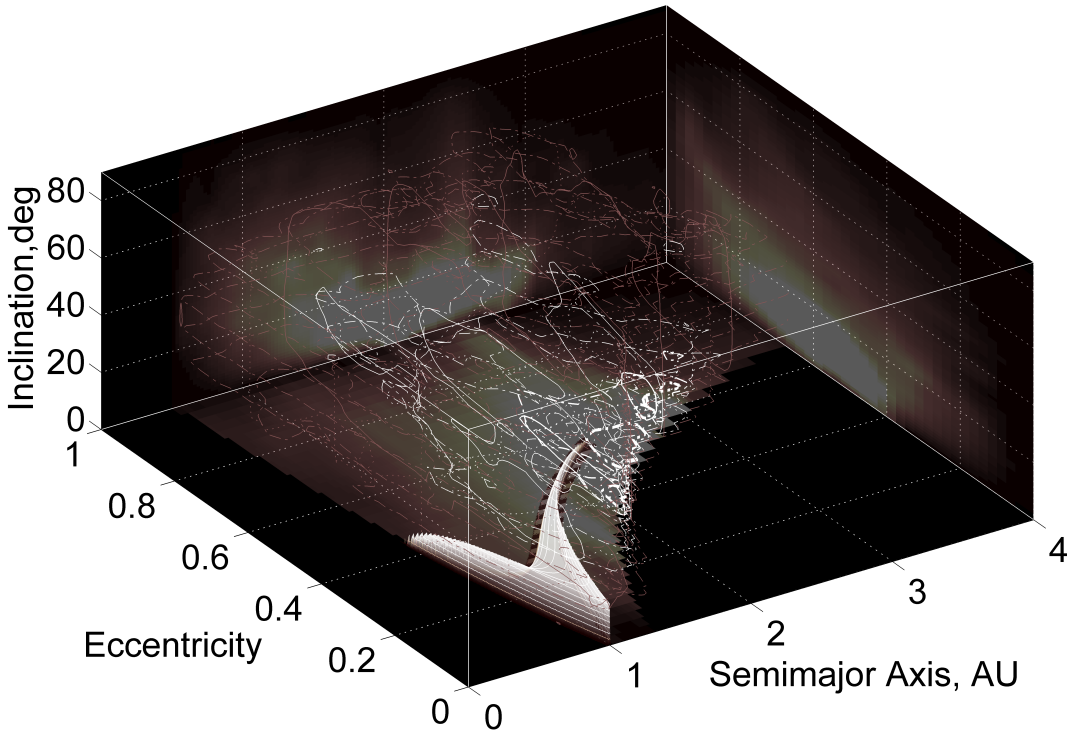

Figure 13. *Accessible region for asteroid exploitation by means of a one-impulse manoeuvre with a 2.37 km/s* Δv *(i.e., v-shaped volume) [33]. Also in the figure, Near-Earth asteroid density distribution represented by a set of isolines within the* $\{a,e\}$ *and* $\{a,i\}$ *planes and cumulative projection of the density at each side wall.*

material. For example, the exploitation of the largest expected object found within a 100 m/s budget, a 24-m asteroid, could supply from 10^7kg to 4×10^7kg of asteroid material, depending on composition and density. If this object was a hydrated carbonaceous asteroid, a million litres of water could possibly be extracted. However, if this object was an M-class asteroid, of order thirty thousand tonnes of metal could potentially be extracted and even a tonne of Platinum Group Metals (PGM). The latter resource could easily reach a value of fifty million dollars in Earth's commodity markets. If the Δv budget is increased to 1 km/s, one 190-m diameter object should be accessible. This corresponds to more than 300 million litres of water or more than 10 million tons of metal and 600 tons of PGMs valued at 30 billion dollars.

4.2 Geo-engineering using captured near Earth asteroids

Another possible use of near Earth asteroids is to provide material for space-based geoengineering schemes. Space-based geoengineering focuses on solar radiation management, i.e., reducing the amount of sunlight reaching the Earth, to create a cooling effect. These methods have either proposed placing large clouds of dust around the Earth or at the $L_4 \backslash L_5$ points in the Earth-Moon system [35] or placing large solar reflectors\refractors at the L_1 point in the Sun-Earth system [1, 28] or also in Earth orbit [30]. In general, the dust cloud methods require much larger total masses due to the dispersed nature of the material, but also because the positions suggested so far mean that for much of the time dust will not be in a position to reflect solar

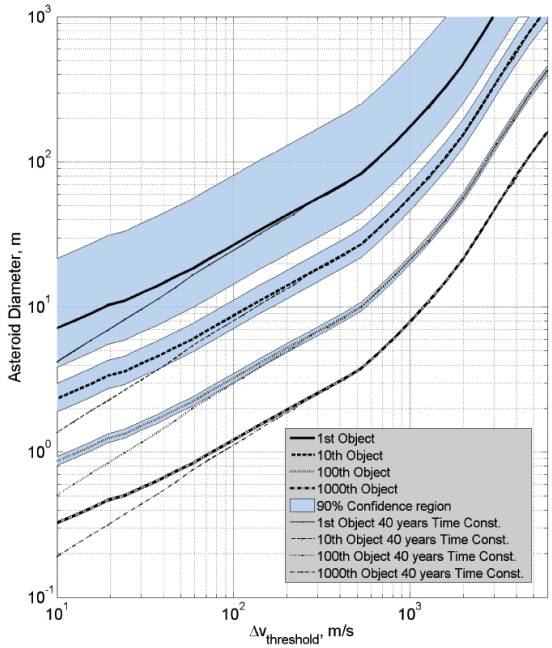

Figure 14. *Expected size of the accessible asteroid.*

photons along the Sun-Earth line.

In contrast, the reflector methods that place objects at the L_1 point are much more mass efficient as the reflectors will constantly be in a position to shade the Earth. However, the downside to this method is that the reflectors must be manufactured either terrestrially and launched into position or manufactured in-situ from captured NEA material. Both of these methods are currently unfeasible due to current launch and space manufacturing capabilities.

Therefore, there is a need to investigate a potentially more near-term method of space-based geoengineering. This is achieved by investigating the macro-scale concept of placing a large cloud of unprocessed asteroid dust at the L_1 point using the micro-scale astrodynamics associated with high area-to-mass ratio particles discussed earlier. It is envisaged that such a dust cloud can be created by either using a solar collector to sublimate material from the surface of a captured NEA, or by mass driver equipped landers on a NEA surface. The sublimation process can be used to both capture the NEA and bound its position in the vicinity of the L_1 point.

In order to model the dynamics of such dust clouds, solar radiation pressure, parameterised by the dust grain 'lightness factor', β, must be included in the equations of motion of the circular restricted three-body problem (CR3BP). The value of β can be determined by the ratio of the solar radiation pressure force to the solar gravitational force and is defined as:

$$\beta = \frac{|F_{rad}|}{|F_g|} = 570\frac{Q}{\rho R} \tag{4}$$

where Q is the coefficient of reflectance, ρ is the grain density in kg m^{-3} and R is the grain radius in μm. The factor Q varies from a value of 0 for a completely transparent material to 1 for a completely absorbing material and 2 for a completely reflecting material. The inclusion of solar radiation pressure results in the effective mass of the Sun being reduced in the mass parameter, μ, as shown in equation (5), thus affecting the dynamics of the CR3BP.

$$\mu = \frac{M_E}{(1-\beta)M_S + M_E} \tag{5}$$

where M_E is the mass of the Earth and M_S is the mass of the Sun. The motion of the particles in the CR3BP can now be modelled for a cloud of dust placed in the region of the interior Lagrange point along the Sun-Earth line, a full description of which can be found in [3]. Due to the instability of the L_1 point, a cloud placed in its vicinity will disperse over time. Using a model of the dynamics of the problem a steady state solution can be found such that the average density of the cloud in the phase space of the problem can be determined for the lifetime of the cloud. Using this understanding of the dust dynamics, along with a solar radiation model, also described in [3], the reduction in solar insolation experienced on the Earth's surface can be determined. This process has been completed for several scenarios which incorporate a varying initial cloud position and size and dust grain size. The initial position varies between the classical L_1 position and the new equilibrium position found when the effect of solar radiation pressure is taken into account, whilst the initial dust cloud radius varies from 500 km to 12,000 km. Four initial grain sizes have also been used, these being 32 μm, 10 μm, 3.2 μm and 0.01 μm, which correspond to β values of 0.005, 0.018, 0.061 and 0.106 respectively [36].

It has been determined that a 1.7% solar insolation reduction will offset the effects of a temperature increase of 2°C [14], equivalent to a doubling of the atmospheric concentration of CO_2. The mass requirement of dust for the cloud being released at the classical L_1 position can be seen in Figure 15 whilst the results for the cloud being released from the new, displaced, equilibrium point

 DOI: 10.2420/AF04.2011.81

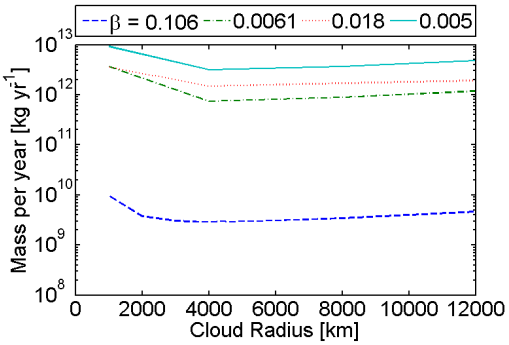

Figure 15. *Mass requirement of dust for the steady state solution of clouds ejected at the* L_1 *point for varying initial cloud radii for the four grain sizes used.*

can be seen in Figure 16. The minimum mass of dust injected into the cloud per year necessary to achieve the required insolation reduction is 8.87×10^8 kg yr^{-1}, as can be seen in Figure 16. This result was achieved for a 3,000 km diameter cloud, released at the displaced equilibrium position for a grain size of 0.01 µm. This mass is considerably lower than previous dust based space-based geoengineering concepts and is also of the same order as the solid reflector methods, assuming a mission lifetime of 10 years, whilst reducing complexity considerably through the use of unprocessed dust rather than highly engineering reflectors or refractors. Further work is being carried out to determine the effect that the gravitational potential of the captured NEA has on the stability of the cloud created from the asteroid. The NEA can therefore help anchor the dust cloud.

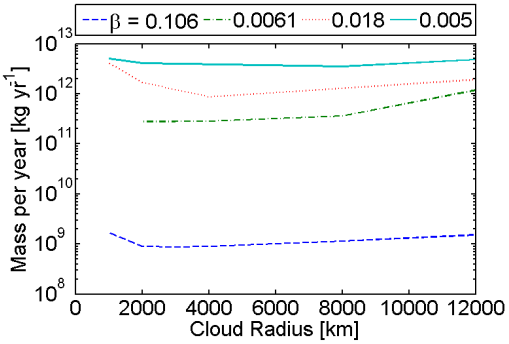

Figure 16. *Mass requirement of dust for the steady state solution of clouds ejected at the new displaced equilibrium points of the four grain radii used for varying initial cloud sizes.*

5 Conclusions

This paper has provided an overview of an on-going programme of work which aims to deliver radically new approaches to astrodynamics at extremes of length-scale to underpin new space-derived products and services. New developments in astrodynamics at three length-scales, micro, meso and macro, have been discussed with a range of applications for future space systems, from space science through to telecommunications and Earth observation, and longer-term concepts such as space-based geo-engineering. A unifying feature of this work is that astrodynamics at the smallest and largest of length-scales will lead to strongly perturbed orbits, for example with MEMS-scale 'smart dust' devices, or natural dust grains, and large gossamer spacecraft. At these extremes of length-scale, perturbations such as atmospheric drag, solar radiation pressure and electrodynamic forces can be of the same order of magnitude as the central two-body or three-body gravitational forces. The strongly perturbed nature of the dynamics of such systems gives rise to rich new families of orbits which can be exploited to deliver new space products and services. Finally, there are intriguing connections between the micro and macro length-scales through the exploitation of an understanding of dust dynamics for both swarms of 'smart dust' and large-scale space-based geo-engineering.

6 Acknowledgments

This work was supported by an Advanced Investigator Grant from the European Research Council through VISIONSPACE (ERC project 227571).

References

[1] R. Angel. Feasibility of cooling the Earth with a cloud of small spacecraft near the inner lagrange point (L_1). *Proceedings of the National Academy of Sciences*, 103(46):17184–17189, 2006.

[2] S. Baig and C. R. McInnes. Light-levitated geostationary cylindrical orbits are feasible. *Journal of Guidance, Control, and Dynamics*, 33(3):782–793, 2010.

[3] R. Bewick, J. P. Sanchez, and C. R. McInnes. An L_1 positioned dust cloud as an effective method of space-based geo-engineering. In *61st International Astronautical Congress (IAC 2010)*, number IAC-10.D1.1.7, 27 September ⊠- 1 October 2010.

[4] W. F. Bottke, A. Morbidelli, R. Jedicke, J. M. Petit, H. F. Levison, P. Michel, and T. S. Metcalfe. Debiased orbital and absolute magnitude distribution of the Near-Earth Objects. *Icarus*, 156(2):399–433, 2002.

[5] M. Ceriotti and C. R. McInnes. An Earth polesitter using hybrid propulsion. In *AIAA/AAS Astrodynamics Specialist Conference*, number AIAA 2010-7830. AIAA, 2-5 August 2010.

[6] M. Ceriotti and C. R. McInnes. Hybrid solar sail and SEP propulsion for novel Earth observation missions. In *61st International Astronautical Congress (IAC 2010)*, number IAC-10.C4.6.8, 27 September – 1 October 2010.

[7] M. Ceriotti and C. R. McInnes. A near term pole-sitter using hybrid solar sail propulsion. In R. Kezerashvili, editor, *2nd International Symposium on Solar Sailing (ISSS 2010)*, pages 163–170. New York City College of Technology, 20-22 July 2010.

[8] C. Colombo, C. M. Lücking, and C. R. McInnes. Orbit evolution, maintenance and disposal of SpaceChip swarms. In *6th International Workshop on Satellite Constellation and Formation Flying (IWSCFF 2010)*, number IWSCFF 2010 2-2, 1-3 November 2010.

[9] C. Colombo and C. R. McInnes. Orbit design for future SpaceChip swarm missions. In *61st International Astronautical Congress (IAC 2010)*, number IAC-10.C1.8.2, 27 September – 1 October 2010.

[10] C. Colombo and C. R. McInnes. Orbital dynamics of Earth-orbiting 'smart dust' spacecraft under the effects of solar radiation pressure and aerodynamic drag. In *AIAA/AAS Astrodynamics Specialist Conference*, number AIAA 2010-7656. AIAA, 2-5 August 2010.

[11] C. Colombo and C. R. McInnes. Orbital dynamics of 'smart dust' devices with solar radiation pressure and drag. *Accepted for publication Journal of Guidance, Control, and Dynamics*, 2011.

[12] J. M. Driver. Analysis of an arctic polesitter. *Journal of Spacecraft and Rockets*, 17(3):263–269, 1980.

[13] G. Gòmez, W. S. Koon, M. W. Lo, J. E. Marsden, J. Masdemont, and S. D. Ross. Connecting orbits and invariant manifolds in the spatial restricted three-body problem. *Nonlinearity*, 17(5):1571–1606, 2004.

[14] B. Govindasamy, K. Caldeira, and P. B. Duffy. Geoengineering Earth's radiation balance to mitigate climate change from a quadrupling of co_2. *Global and Planetary Change*, 37(1-2):157–168, 2003.

[15] J. Heiligers. Displaced geostationary orbits using hybrid low-thrust propulsion. In *61st International Astronautical Congress (IAC 2010)*, number IAC-10-E2.1.2, 2010.

[16] IPCC. Contribution of working groups i, ii and iii to the fourth assessment report of the intergovernmental panel on climate change. *Core Writing Team, Pachauri, R.K. and Reisinger, A. (Eds.), IPCC, Geneva, Switzerland. pp 104*, 2007.

[17] R. Jehn, A. Rossi, T. Flohrer, and D. Navarro-Reyes. Reorbiting of satellites in high altitudes. In *5th European Conference on Space Debris*, 2009.

[18] D. King-Hele. *Theory of satellite orbits in an atmosphere*. Butterworths, London, 1964.

[19] W. S. Koon, M. W. Lo, J. E. Marsden, and S. D. Ross. Heteroclinic connections between periodic orbits and resonance transitions in celestial mechanics. *Chaos*, 10(2):427–469, 2000.

[20] M. A. Lazzara. The polar meteorlogist's dream machine: artificial Lagrange orbit satellite applications via arctic and antarctic composite satellite

 DOI: 10.2420/AF04.2011.81

imagery. In R. Kezerashvili, editor, *2nd International Symposium on Solar Sailing (ISSS 2010)*, pages 49–55. New York City College of Technology, 20-22 July 2010.

[21] M. Leipold and M. Götz. Hybrid photonic/electric propulsion. Technical Report SOL4-TR-KTH-0001, ESA contract No. 15334/01/NL/PA, Kayser-Threde GmbH, Jan. 2002. ESA contract No. 15334/01/NL/PA.

[22] J. Lewis. *Mining the sky: untold riches from asteroids, comets and planets*. Helix Books/Perseus Books Reading, 1996.

[23] C. M. Lücking, C. Colombo, and C. R. McInnes. Orbit control of high area-to-mass ratio spacecraft using electrochromic coating. In *61st International Astronautical Congress (IAC 2010)*, number IAC-10.C1.2.7, 27 September – 1 October 2010.

[24] M. Macdonald and C. R. McInnes. Solar sail mission applications and future advancement. In R. Kezerashvili, editor, *2nd International Symposium on Solar Sailing (ISSS 2010)*, 2010.

[25] C. R. McInnes. The existence and stability of families of displaced two-body orbits. *Celestial Mechanics and Dynamical Astronomy*, 67(2):167–180, 1997.

[26] C. R. McInnes. Dynamics, stability, and control of displaced non-Keplerian orbits. *Journal of Guidance, Control, and Dynamics*, 21(5):799–805, 1998.

[27] C. R. McInnes. *Solar Sailing: Technology, Dynamics and Mission Applications*. Springer-Praxis Books in Astronautical Engineering, Springer-Verlag, 1999.

[28] C. R. McInnes. Space-based geoengineering: challenges and requirements. *Proceedings of the Institution of Mechanical Engineers, Part C: Journal of Mechanical Engineering Science*, 224(3):571–580, 2010.

[29] O. Mori, H. Sawada, R. Funase, T. Endo, M. Morimoto, T. Yamamoto, Y. Tsuda, Y. Kawakatsu, and J. Kawaguchi. Development of first solar power sail demonstrator - IKAROS. In *21st International Symposium on Space Flight Dynamics (ISSFD 2009)*. CNES, 2009.

[30] J. Pearson, J. Oldson, and E. Levin. Earth rings for planetary environment control. *Acta Astronautica*, 58(1):44–57, 2006.

[31] A. E. Roy. *Foundations of Astrodynamics*. Macmillan, London, 1965.

[32] J. P. Sanchez, C. Colombo, M. Vasile, and G. Radice. Multi-criteria comparison among several mitigation strategies for dangerous Near Earth Objects. *Journal of Guidance, Control and Dynamics*, 32(1):121–142, 2009.

[33] J. P. Sanchez and C. R. McInnes. Assessment on the Feasibility of Future Sheperding of Asteroid Resources. In *61st International Astronautical Congress (IAC 2010)*, number IAC-10.D3.2.7. International Astronautical Federation, 27 September 1 October 2010.

[34] J. Shepherd, K. Caldeira, P. Cox, and J. Haigh. Geoengineering the climate. *Report of Royal Society working group of geo-engineering*, 2009.

[35] C. Struck. The feasibility of shading the greenhouse with dust clouds at the stable lunar Lagrange points. *Journal of the British Interplanetary Society*, 60(3):82–89, 2007.

[36] M. Wilck and I. Mann. Radiation pressure forces on "typical" interplanetary dust grains. *Planetary and Space Science*, 44(5):493–499, 1996.